AGU PUBLICATIONS

JGR

Journal of Geophysical Research: Atmospheres

RESEARCH ARTICLE
10.1002/2015JD024547

Key Points:
- Detection of meteor head echoes through HPLA radars
- Minimization of ablation equations to calculate neutral densities and ablation parameters
- Error roughly 10%–12% across binned estimates

Correspondence to:
A. Li,
alanli@stanford.edu

Citation:
Li, A., and S. Close (2016), Neutral density estimation derived from meteoroid measurements using high-power, large-aperture radar, *J. Geophys. Res. Atmos.*, *121*, 8023–8037, doi:10.1002/2015JD024547.

Received 24 NOV 2015
Accepted 30 MAY 2016
Accepted article online 7 JUN 2016
Published online 4 JUL 2016

Neutral density estimation derived from meteoroid measurements using high-power, large-aperture radar

A. Li[1] and S. Close[1]

[1] Department of Aeronautics and Astronautics, Stanford University, Stanford, California, USA

Abstract We present a new method to estimate the neutral density of the lower thermosphere/upper mesosphere given deceleration measurements from meteoroids as they enter Earth's atmosphere. By tracking the plasma (referred to as head echoes) surrounding the ablating meteoroid, we are able to measure the range and velocity of the meteoroid in 3-D. This is accomplished at Advanced Research Projects Agency Long-Range Tracking and Instrumentation Radar (ALTAIR) with the use of four additional receiving horns. Combined with the momentum and ablation equations, we can feed large quantities of data into a minimization function which estimates the associated constants related to the ablation process and, more importantly, the density ratios between successive layers of the atmosphere. Furthermore, if we take statistics of the masses and bulk densities of the meteoroids, we can calculate the neutral densities and its associated error by the ratio distribution on the minimum error statistic. A standard deviation of approximately 10% can be achieved, neglecting measurement error from the radar. Errors in velocity and deceleration compound this uncertainty, which in the best case amounts to an additional 4% error. The accuracy can be further improved if we take increasing amounts of measurements, limited only by the quality of the ranging measurements and the probability of knowing the median of the distribution. Data analyzed consist mainly of approximately 500 meteoroids over a span of 20 min on two separate days. The results are compared to the existing atmospheric model NRLMSISE-00, which predicts lower density ratios and static neutral densities at these altitudes.

1. Introduction

Prediction of atmospheric density variations within the mesosphere/lower thermosphere (MLT) (roughly 50–120 km) region has been a challenge to the atmospheric science and space community for the past 50 years. The study of this region gives insights to the dynamical processes active within our atmosphere, as well as enabling accurate prediction of the motion of objects in this area (deorbiting satellites and rocket bodies). Atmospheric density itself is a complex phenomenon that varies spatially and temporally and is inherently linked with the behavior of the Sun [*Vallado*, 2013, pp. 553–555]. Moreover, coupling between different layers as well as varying scale processes ranging from centimeters up to thousands of kilometers make the entire system very difficult to model [*Holten*, 2012].

Despite the difficulties, there have been many models developed to predict mass density. Semiempirical models, such as the Jacchia and Mass Spectrometer and Incoherent Scatter (MSIS) series [*Jacchia*, 1965; *Hedin*, 1987; *Picone et al.*, 2002; *Bowman et al.*, 2008], take data collected from various satellites and instruments to fit a parameterized mathematical formulation of the atmosphere. These models initially start as a model of atmospheric temperature and use the $F_{10.7}$ and K_p indices as inputs, where the former is a measure of extreme ultraviolet (EUV) irradiance responsible for atmospheric heating and the latter the energy associated with geomagnetic activity. These models are widely used for benchmarking and parameter retrieval purposes, with the oft cited 15% error associated with these estimates [*Pardini and Anselmo*, 2001; *Vallado and Finkleman*, 2014]. It has been shown that errors can reach as high as even 20–50% during turbulent periods of high solar activity [*Doornbos*, 2012]. Alternatively, physical models attempt to numerically solve fluid equations from first principles, with attempts to incorporate all the intricacies inherent in the atmosphere (e.g., heating and cooling processes, species-specific reaction rates, and gravity waves) [*Akmaev*, 2011]. These models can simulate new geophysical conditions lacking in historical data, but due to the increased complexity and dependence

on external drivers, their predictive capabilities are relatively on par with empirical models [*Shim et al.*, 2012]. A comprehensive review of all these models can be found in [*Emmert*, 2015].

To verify and calibrate the aforementioned models, the most direct method is to perform in situ measurements utilizing instrumentation aboard sounding rockets and satellites. Neutral mass spectrometers (NMS) have been deployed on various missions to determine the specific composition and number densities of the atmosphere's constituents [*Offerman*, 1974; *Hedin*, 1987]. Accelerometers have also been used to measure the nonconservative effects of drag, but the use of these in the MLT region have been brief and intermittent [*Champion and Marcos*, 1973]. Other methods include the use of pressure and ionization gauges, with typical errors of roughly 2% [*Clemmons et al.*, 2008; *Strelnikov et al.*, 2013]. All these sensors are able to provide a direct measure of the properties of the atmosphere, but since they require expensive and high-quality instrumentation, missions involving them are infrequent and sparse.

Recently, developments in remote sensing have allowed new nonintrusive methods of determining mass densities. One such method is to observe the infrared airglow below 110 km to infer the quantities of anomalous oxygen (O) present [*Grossmann et al.*, 2000]. Another promising method involves atmospheric occultation, where by measuring the attenuation of IR, UV, and X-ray sources, we can determine the composition as well as the total mass density of the MLT region [*Meier et al.*, 1992; *Determan et al.*, 2007]. Finally, closer to the content of this paper is the use of incoherent scatter radar (ISR) data to investigate neutral atmospheric variations [*Nicolls et al.*, 2014].

This paper defines a new technique using high-power, large-aperture (HPLA) radars to observe vast quantities of incoming meteoroids within Earth's atmosphere. Coupled with a few physical laws relating the deceleration and ablation of these meteoroids, we take a data-driven approach to determine MLT neutral densities in a region where measurements are relatively scarce. The paper is organized as follows: Section 2 describes the properties of micrometeoroids and its associated radar data, section 3 describes the procedure to estimate the neutral densities, section 4 presents the results of this analysis from the Advanced Research Projects Agency Long-Range Tracking and Instrumentation Radar (ALTAIR), and finally, section 5 will outline conclusions and future work.

2. Meteoroids and Radar Data

Meteoroids are classified as small bodies moving within the solar system that are much smaller than asteroids. The cumulative number of these meteoroids increases exponentially as the mass decreases [*Grun et al.*, 1985; *Divine*, 1993]. Moreover, measurements from the Long Duration Exposure Facility (LDEF) satellite have estimated that the mass deposited from the smallest particles (<1 mm in diameter) is comparable to or greater than that deposited from larger bodies over 1 cm in size [*Love and Brownlee*, 1993]. This research focuses on the smallest subclass of meteoroids, often referred to as "micrometeoroids." There are two particular sources of meteoroids: "streams," which is the result of the Earth passing through the tail of a comet or asteroid, and "sporadics," where the meteoroid has lost the identity of its parent's orbit. Often streams are linked with meteor showers, while sporadics are considered to be always present in the background. This paper focuses on the latter of the two, with measurements made away from shower events.

When a meteoroid enters the Earth's atmosphere, it is subject to a number of physical processes as it collides with molecules within Earth's atmosphere. Chief among these interactions is the meteoroid's deceleration and its ablation, the latter of which is defined as the removal of the meteoroid mass via phase transformations as its temperature increases. The ablation process is a complicated phenomenon and has been studied and modeled extensively [*Vronshten*, 1983; *Ghosh and McSween*, 1999; *Popova*, 2004; *Vondrak et al.*, 2008; *Briani et al.*, 2013]. It is dependent upon many factors such as the meteoroid's composition, mass, entry angle, and velocity as well as atmospheric conditions. As the meteoroid ablates, its material ionizes and creates a plasma that surrounds the meteoroid (termed as head echoes) and moves with the velocity of the meteoroid; these are easily detected using HPLA radars. For our purposes, we will take the popular assumption that the meteoroid travels at the velocity of the head echo [*Chau et al.*, 2007; *Kero et al.*, 2012], although there have been doubts related to this assumption [*Simek et al.*, 1997].

The use of radars to collect meteor data has been well established since the late 1940s [*Hey et al.*, 1946], but the HPLA radars have yielded significant insights into the field of meteor physics [*Pellinen-Wannberg and Wannberg*, 1994; *Janches et al.*, 2000; *Close et al.*, 2000; *Mathews et al.*, 2001; *Oppenheim et al.*, 2008]. In particular,

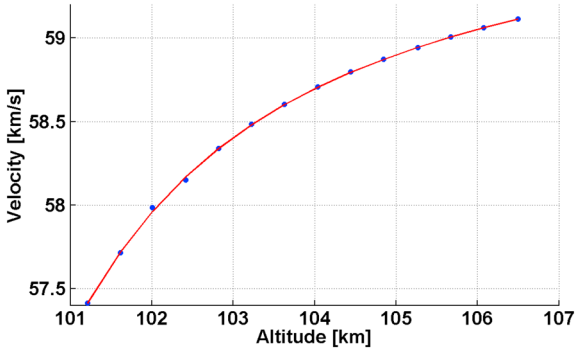

Figure 1. Fitting of velocity data versus altitude as a sum of two exponentials. The acceleration is calculated as $\frac{dv}{dh}\frac{dh}{dt}$. Errors in range rate $\frac{dh}{dt}$ are considered small. Adjusted $R^2 = 0.9997$ and RMSE = 0.0088.

because of their ability to directly observe the velocity and deceleration of the head echo target, the masses and bulk densities of meteoroids can be derived [*Close et al.*, 2005, 2012]. Since atmospheric density is a major component to these calculations, meteoroids have been used as probes for atmospheric science before the advent of in situ monitoring [*Opik*, 1958]. Likewise, assumptions regarding atmospheric densities directly affect derived meteor properties as well [*Lyytinen and Gritsevich*, 2016].

The radar used in this study is ALTAIR, which is a 46 m diameter HPLA radar that is located on the Kwajalein Atoll at 9°N and 167°E. It transmits at a peak power of 6 MW simultaneously at two frequencies with right circularly (RC) polarized signal energy in a half-power beam width of 2.8° and 1.1° at VHF and UHF (typical operating frequencies are 160 MHz and 422 MHz), respectively. ALTAIR receives both right-circular and left-circular (LC) energy and has four additional receiving horns for the purpose of angle measurement, which gives the position, velocity, and deceleration of an object in three dimensions.

Radar meteor data were collected simultaneously at VHF and UHF at ALTAIR in 2007 and 2008 and include approximately 30 h of data. In particular, amplitude and phase data from meteoroid head echoes and trails were observed in each frequency and four receiving channels for altitudes spanning 80–140 km. The two ALTAIR waveforms used to collect the data were a 100 μs VHF chirped pulse ("V7100") and a 150 μs UHF chirped pulse ("U7100"), both with 15 m range spacing. These waveforms were chosen for their high sensitivity and range resolution. A 115 Hz pulse repetition frequency (PRF) was utilized due to ALTAIR system requirements associated with these two waveforms. With this, ALTAIR can detect a target as small as −50 decibels relative to a square meter (dBsm) at VHF and −65 dBsm at UHF at a range of 100 km [*Janches et al.*, 2008].

Delaunay triangulation was used to automatically detect head echoes within the 30 h of data [*Close et al.*, 2012]. The head echo range rates and 3-D speeds were derived by applying a phase-derived matching technique, described in [*Loveland et al.*, 2011], which reduces the range rate error to the order of 1 m/s. The errors in the monopulse can be assumed to be on average 11.2 mdeg in azimuth and elevation [*Brown et al.*, 2001], which at a range of 100 km gives an average velocity error of 2.3 km/s in the worst case for meteoroids traveling completely perpendicular to the radar boresight. This equates to an error of less than 6% for meteoroids traveling over 40 km/s, which we actively filter for (details in section 4). The acceleration error is more difficult to quantify, as the interpulse timing of 8.7 m s makes finite differencing inaccurate. In the best case scenario for meteoroids traveling "down the beam," finite differencing leads to an acceleration error of approximately 4%. We thus model the velocity versus altitude from a meteoroid streak as the sum of two exponential functions, with an average $R^2 \approx 0.99$ and root-mean-square error (RMSE) ≈ 0.023 (see Figure 1). Acceleration is taken as the product between the derivative of the function with respective to altitude ($\frac{dv}{dh}$) with the change in altitude ($\frac{dh}{dt}$), which is closely related to the range rate.

The majority of the data analyzed consists of two continuous sets of observations on two different days approximately 20 min each: 1800 UTC, day 312, 2007 and 1800 UTC, day 15, 2008, respectively. Thegeomagnetic conditions on these two days are outlined in Table 1. The data sets on these two days were chosen for their continuity and quantity of observations, as well as the local time being favorable for the detection of apex meteoroids traveling down the radar beam. Analysis on day 131, 1600 UTC, 2007, is meant to serve as a introduction to the methodology, which unfortunately due to the lack of further data on this day makes cross validation of the methodology difficult.

Table 1. $F_{10.7}$ Index for Solar Irradiance and K_p Index for Geomagnetic Activity on Analyzed Days

Day	$F_{10.7}$	$F_{10.7,81\text{dayavg}}$	K_p
312	70	72	1−
015	74	75	2+

Table 2. List of Variables and Respective Comments[a]

Variable	Comments	Solve for?
V - Velocity	Data observed from head echoes	No
M - Mass	Taken from statistics to solve for actual densities (see section 3.2)	No
ρ_m - Meteoroid bulk density	Taken from statistics to solve for actual densities (see section 3.2)	No
A - Frontal Area	Related to radius	No
R - Radius	Related to mass and bulk density	No
C_D - Drag coefficient	Often assumed = 2, combined into D, and held constant	?
C_H - Heat transfer coefficient	Often assumed = 1, combined into D, and held constant	?
H^* - Heat of enthalpy	Combined into D and held constant	?
D - Ablation parameter	$D = \frac{1}{6}\frac{C_H}{C_D H^*}$ and held constant	Yes
ρ_a - Atmospheric density	Main solve for variable	Yes

[a]Note that the question mark indicates that the variable can either take the assumed value or can be treated as an unknown but not explicitly solved for. Instead D, the ablation parameter which is a combination of these unknowns, is solved for instead.

3. Methodology

3.1. Density Ratios

When the meteoroid and air molecules collide, the conservation of linear momentum (neglecting external forces) is described by

$$\vec{a}_D = \frac{d\vec{V}_{rel}}{dt} = -\frac{1}{2} C_D \frac{A}{M} \rho_a V_{\text{rel}}^2 \frac{\vec{V}_{\text{rel}}}{\left|\vec{V}_{\text{rel}}\right|} \tag{1}$$

where $\vec{a}_D$ is the (negative) acceleration due to drag, C_D the drag coefficient, A the object's exposed cross-sectional drag area, M the object mass, ρ_a the atmospheric density, and $\vec{V}_{\text{rel}}$ the relative velocity of the object to the atmosphere. In meteoroid literature, (1) is often simplified to

$$\frac{dV}{dt} = -\frac{1}{2}\frac{C_D A \rho_a V^2}{M} \tag{2}$$

where we take the motion tangent to the trajectory to relieve the vector notation. Often in meteoroid literature, the substitution $\Gamma = \frac{1}{2} C_D$ is made. Note that in this formulation, we neglect gravity and the relative velocity of the atmosphere due to their negligible contributions as well as higher order terms that result from the momentum equation. We also assume that the meteoroid travels linearly along its trajectory during the duration of detection.

The second fundamental equation relates to the mass loss of the meteoroid due to ablation:

$$\frac{dM}{dt} = -\frac{1}{2}\frac{C_H}{H^*} \rho_a A V^3 \tag{3}$$

where C_H is the heat transfer coefficient and H^* the heat of enthalpy (otherwise known as latent heat of vaporization, sublimation, or fusion). Equations (2) and (3) contain many subtleties, a major one being that the variables C_D, C_H, and H^* are not truly constant over the meteoroid's lifetime. Moreover, differential ablation may contribute to different rates of sublimation across the meteoroid's surface and alter its assumed spherical shape [*Janches et al.*, 2009]. However, for our purposes, we will take these variables as constant over short observed time spans. Table 2 shows the relevant variables within this paper and the assumptions of each.

If we divide (3) by (2), we can form the differential equation:

$$\frac{1}{M}\frac{dM}{dt} = \frac{C_H}{C_D H^*} V \frac{dV}{dt} \tag{4}$$

If we know the initial mass M_0 and velocity V_0 of the meteoroid at the start of detection, and take C_H, C_D, and H^* as constants, we arrive at the following relation:

$$M = M_0 e^{\frac{C_H}{2 C_D H^*}(V^2 - V_0^2)} \tag{5}$$

Moreover, if we assume a constant spherical profile of the ablating meteoroid, Equation (5) becomes:

$$R = R_0 e^{\frac{C_H}{6C_D H^*}(V^2 - V_0^2)} \tag{6}$$

where R is the radius of the meteoroid. Since we assume isothermal heating for small meteoroids, the constant spherical shape factor assumption is valid *Rogers et al.* [2005].

The same spherical assumption can be applied to equation (2):

$$\frac{1}{V^2}\frac{\mathrm{d}V}{\mathrm{d}t} = -\frac{3}{8}\frac{C_D \rho_a}{\rho_m R} \tag{7}$$

where ρ_m is the bulk density of the meteoroid. If we take the logarithm of the ratio of equation (7) between two distinct points in time (t_1 and t_2) for a certain meteoroid, we get

$$\ln\left(\frac{1}{V_2^2}\frac{\mathrm{d}V_2}{\mathrm{d}t}\right) - \ln\left(\frac{1}{V_1^2}\frac{\mathrm{d}V_1}{\mathrm{d}t}\right) = D\left(V_1^2 - V_2^2\right) + \ln\left(\frac{\rho_{a2}}{\rho_{a1}}\right) \tag{8}$$

where we abbreviate $D = \frac{1}{6}\frac{C_H}{C_D H^*}$. Note that equation (8) relates the observations of the velocity and deceleration of the meteoroid with the unknown constants as well as a density ratio parameter. Also, we have taken an approach where the atmosphere is divided into successive layers and each layer is approximated to possess its own constant neutral density. Furthermore, we can relate velocity to altitude with the following identity:

$$\frac{\mathrm{d}z}{\mathrm{d}t} = -V\sin\gamma \tag{9}$$

where z is the altitude and γ the angle at which the meteoroid is approaching at.

In general, we can write equation (8) for the ith meteoroid at the jth altitude as

$$F_{i,j} = D_i W_{i,j} + \ln\left(\rho_{rj}\right) \tag{10}$$

where

$$F_{i,j} = \ln\left(\frac{1}{V_{i,j+1}^2}\frac{\mathrm{d}V_{i,j+1}}{\mathrm{d}t}\right) - \ln\left(\frac{1}{V_{i,j}^2}\frac{\mathrm{d}V_{i,j}}{\mathrm{d}t}\right)$$

$$W_{i,j} = \left(V_{i,j}^2 - V_{i,j+1}^2\right)$$

$$\rho_{rj} = \frac{\rho_{a,j+1}}{\rho_{a,j}}$$

Equation (10) takes successive ratios between the jth layer of the atmosphere with the next $(j+1)$th layer, but this formulation can easily be altered such that the ratio is between one layer of the atmosphere with a particular reference layer. The advantage of the former formulation is that we incorporate more measurements within our minimization scheme since not all meteoroids are observed throughout all layers, while the latter formulation requires all the analyzed meteoroids to pass through similar layers. However, with the latter method we are more consistent since we ensure that there is an equal number of meteoroid measurements across all altitudes and avoid areas where data might be lacking. This paper will focus on the former method so as to leverage more data within the minimization scheme. Note that D_i in equation (10) is the unknown but constant ablation parameter per meteoroid.

Continuing with the successive ratio formulation, equation (10) can easily be manipulated into the matrix form for the ith meteoroid:

$$\begin{bmatrix} F_{i,1} \\ F_{i,2} \\ \vdots \\ F_{i,m} \end{bmatrix} = \begin{bmatrix} I_{i,j=1} & 0 & \cdots & 0 & W_{i,1} \\ 0 & I_{i,j=2} & \cdots & 0 & W_{i,2} \\ \vdots & \vdots & \ddots & \vdots & \vdots \\ 0 & 0 & \cdots & I_{i,j=m} & W_{i,m} \end{bmatrix} \begin{bmatrix} \ln(\rho_{r1}) \\ \ln(\rho_{r2}) \\ \vdots \\ \ln(\rho_{rm}) \\ D_i \end{bmatrix} \tag{11}$$

Here we have used the indicator notation such that $I_{i,j=k}=1$ if there is data for the ith meteoroid at the kth altitude, and $I_{i,j=k}=0$ otherwise. Note that by this logic, there are instances where $F_{i,k}=0$ and $W_{i,k}=0$ if there is no data available for the ith meteoroid at the kth altitude. In these cases, rows consisting of entirely zeros can be neglected. In essence, we have split the atmosphere into $m+1$ layers and make observations from a total of n meteoroids. Ideally, if all meteoroids travel through all $m+1$ altitudes, then we would be estimating $m+n$ parameters from $m \cdot n$ equations.

We estimate the unknowns ρ_{rj} and D_i by solving

$$\begin{aligned} &\text{minimize} \quad \sum_{i,j} \left| F_{i,j} - D_i W_{i,j} - \ln(\rho_{rj}) \right| \\ &\text{subject to} \quad D_i > 0 \end{aligned} \tag{12}$$

Note that equation (12) is convex and hence possesses a global minimum. We choose the 1 norm over the 2 norm as to reject outliers (meteoroids that do not conform to our ablation model) and impose the positive restriction $D_i > 0$ such that the results are physical.

3.2. Density Values

If we take the ratio of equation (7) again between two arbitrary meteoroids (1 and 2) at the start of their ablation processes, we get

$$\frac{\frac{dV_2}{dt}\frac{1}{V_2^2}}{\frac{dV_1}{dt}\frac{1}{V_1^2}} = \frac{R_1 \rho_{m1} \rho_{a2}}{R_2 \rho_{m2} \rho_{a1}} \tag{13}$$

Since the meteoroids might initially be detected at different altitudes, the density ratio $\frac{\rho_{a2}}{\rho_{a1}}$ is appended to the end of the equation. However, having solved for the density ratios in the previous section, we can compare all densities to a reference density, $\rho_{a,\mathrm{ref}}$:

$$\frac{\frac{dV_2}{dt}\frac{1}{V_2^2}\frac{\rho_{a,\mathrm{ref}}}{\rho_{a2}}}{\frac{dV_1}{dt}\frac{1}{V_1^2}\frac{\rho_{a,\mathrm{ref}}}{\rho_{a1}}} = \frac{R_1 \rho_{m1}}{R_2 \rho_{m2}} = \frac{K_1}{K_2} \tag{14}$$

Note that we can calculate K from the observed velocity, deceleration, and atmospheric density ratios. This in turn relates directly to the radius and bulk density of the meteoroid. Because errors in the measurements directly translate into erroneous ratios across K, this impacts on the supposed distribution of $R\rho_m$. This effect can be accounted for if we know the error associated with the measurements and if it is assumed Gaussian.

Here we turn to the method of order statistics to approach the problem from a stochastic perspective. The method is outlined in *Li and Close* [2015] as it relates to satellites but can be reworked such that it applies to meteoroids as well. We will give a brief outline of the method here, with the details given in Appendix A.

To utilize order statistics, we first require a larger pool of data points such that we can form meaningful statistics. Because of the large variation across individual meteoroids, it is advantageous to amalgamate measurements across multiple hours or even days. A dilemma arises during this procedure since neutral density is a varying phenomenon, and hence, calculating individual K values for a particular time period is ultimately biased toward the neutral densities present at that time. This is remedied as shown in equation (14), where when we take ratios of measurements associated with a certain time, we negate the effects of neutral density bias.

We define the minimum K value among n meteoroids per time frame as

$$K_{mk}(t_k) = \min_n K_n(t_k) \tag{15}$$

and hence can reformulate equation (14) as

$$\frac{K_j(t_k)}{K_{mk}(t_k)} = \frac{(R\rho_m)_j}{(R\rho_m)_{mk}} \tag{16}$$

We can take equation (16) and construct the cumulative distribution function (CDF) of the ratio distribution on the minimum order statistic by collecting data across multiple time frames. Although we are able to cancel

out biases of varying densities with this method, a major assumption here is that the meteoroids must all be independent and identically distributed (IID) according to the same distribution across all time periods. This assumption is valid if we make measurements across smaller time scales such as an hour or across similar local times spanning over multiple days if we expect the same sporadic background of meteoroids to be present. Care must be taken while combining measurements as to ensure the IID assumption is consistent.

The CDF associated with the meteoroid size and bulk density can be inferred from the constructed ratio CDF mentioned previously. This is done by solving

$$\frac{n-1}{n}\left(\begin{bmatrix} C_m \\ C_{m-1} \\ \vdots \\ C_2 \end{bmatrix} - 1\right) = \begin{bmatrix} F_m & 0 & \cdots & 0 \\ F_{m-1} & F_m & \cdots & 0 \\ \vdots & \vdots & \ddots & \vdots \\ F_2 & F_3 & \cdots & F_m \end{bmatrix} \begin{bmatrix} F_2^{n-1} - F_1^{n-1} \\ F_3^{n-1} - F_2^{n-1} \\ \vdots \\ F_m^{n-1} - F_{m-1}^{n-1} \end{bmatrix} \tag{17}$$

where C_i is the constructed ratio CDF from equation (16) and F_i is the complement of the CDF we must solve for, both evaluated at prescribed geometric intervals. It must be pointed out that equation (17) is inherently an integral equation solved numerically, and hence, an ambiguous integration constant results from the process. This constant can be evaluated if we know the median of the distribution beforehand with some associated probability. The detailed derivation of (17) is given in Appendix A.

Given the CDF of $(R\rho_m)$, we can proceed to calculate the neutral density at the reference altitude:

$$\rho_{a,\mathrm{ref}} = -\frac{8}{3}\frac{(R\rho_m)}{C_D V^2}\frac{\mathrm{d}V}{\mathrm{d}t}\frac{\rho_{a,\mathrm{ref}}}{\rho_a} \tag{18}$$

The densities at other altitudes can simply be calculated by multiplying equation (18) with the density ratios derived in section 3.1. Also, we can see that if we possess the error characteristics of $(R\rho_m)$ from its CDF, we can put associated error bounds on the estimated $\rho_{a,\mathrm{ref}}$. If we thicken the atmospheric layers, the assumption of a constant density per layer becomes increasing invalid, to the point that each layer differs from the previous by large margins. Conversely, thinning the layers is limited by the velocity data available to us, and thus, we introduce additional error from needing to interpolate an increasing number of points. Additional errors in velocity (V) and, more importantly, deceleration $\left(-\frac{\mathrm{d}V}{\mathrm{d}t}\right)$, also propagate into the calculation of neutral density.

There are a few embedded assumptions within the entire estimation process, which we will now address. Besides for the IID assumption, we have assumed that the ablation process starts at the first detection point of the meteoroid. The statistics of the meteoroids' sizes and bulk densities pertains to their exospheric characteristics, but a meteoroid might have begun ablating earlier only to cross the radar beam afterward. This can be accounted for by selecting meteoroids where the deceleration begins at approximately zero with a low RCS to indicate relatively little to no starting ablation. Care must be taken to accurately remove the beam pattern from RCS data, since the RCS or SNR variation with range/time is primarily due to the particle traversing the radar beam.

Another assumption is the constant properties (C_H, H^*, and C_D) of the ablating meteoroid mentioned in section 3.1, which holds true for short duration observations over specific portions of the ablating meteoroid's lifetime (most meteoroids were observed for < 1 s). Although this implies that not all meteoroids traverse all layers of the atmosphere, recall that this is unnecessary in estimating the densities, since all we require is that the cumulative number of all meteoroids traverses all the appropriate altitudes.

Finally, erroneous or noisy measurements of the meteoroids' velocity and deceleration can lead to incorrect estimates of the neutral densities and its ratios. This inconsistency can be checked if we are able to divide the data gathered over a particular time frame into separate bins and evaluate each bin independently. The normalized error of equation (12) can be calculated to determine how well the estimated densities based upon the model match observational data.

4. Results

The methodology presented in the previous section is applied to ALTAIR data collected throughout 2007–2008. We restrict our observations to VHF detections since they tend to possess higher RCS values and longer durations due to a wider beam. We filter our results such that we discount very short duration observations (<0.05 s) and low-velocity meteoroids (< 40 km/s). Longer duration observations have the following advantages:

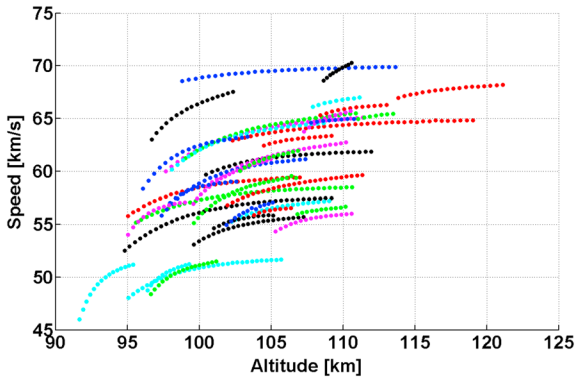

Figure 2. Meteoroid speeds > 40 km/s as detected by ALTAIR. Each color represents a separate meteoroid event (note that colors are reused). Data taken are at 1600 UTC, day of year (DOY) 131, 2007, spanning over approximately 3 min.

1. They generally are coming down the beam parallel to the radar boresight instead of traversing across the beam, and hence, the monopulse error is minimized. As most of the sporadics come from the ecliptic plane, this holds true for ALTAIR, which is close to the equator.
2. The meteoroid is more likely to be genuine and contains more material, as shorter duration observations tend to be small/weak with a low SNR.
3. They tend to traverse more layers of the atmosphere.
4. Less likelihood of anomalous physics that we are not modeling (such as flares or breakups) [*Baldwin and Sheaffer*, 1971; *Rogers et al.*, 2005; *Janches et al.*, 2009].

As well, in choosing higher-velocity meteoroids, the deceleration is more evident. However, there exists a mass-velocity selection effect associated with any plasma detection such that it is insensitive to both low-mass, low-velocity meteoroids and low-mass, high-velocity meteoroids (i.e., almost no meteoroids below 1×10^{-7} g in mass and over 70 km/s are observed) *Close et al.* [2007].

Figure 2 shows the 3-D speeds (>40 km/s) of 38 meteoroids detected over approximately 2 min. Figure 3 shows the deceleration multiplied by $\frac{1}{V^2}$ of the same meteoroids (refer to equation (7)). In both cases, the deceleration is quite evident as the meteoroid traverses lower in altitude where the neutral density exponentially increases.

If we apply the minimization of equation (12) to the deceleration data, the resulting density ratio $\frac{\rho_a}{\rho_{a,110\text{km}}}$ is shown in Figure 4. Comparisons are made to the NRLMSISE-00 and exponential (8 km scale height, hydrostatic equilibrium) models. However, we have not yet addressed the matter of consistency of our data-driven scheme, as noisy or incomplete data could corrupt or produce erroneous results. Furthermore, if we desire actual density values instead of ratios, we must start amalgamating ratio statistics while keeping with the IID assumption of incoming meteoroids. Both these problems can be remedied by binning data over a longer period into multiple sets and evaluating each set independently.

The result of taking data over 20 min and binning it into nine equal intervals is shown in Figures 5 and 6. Because we take data from a short time interval, we can be fairly certain that the observed meteoroids follow the same distribution and that the background neutral density remains fairly constant (given that geomagnetic indices are only updated every 3 h, this is a good assumption). This actually negates the need to amalgamate ratio statistics since the method is primarily designed to counter the effects of changing atmospheric densities. We can see then from Figures 5 and 6 that estimates with high mean squared error generally lie as outliers and hence are not good predictors. Note that the method is not without false positives and false negatives. An example of the former can be found in Figure 6 as a prediction with large error located close to the predicted mean, and an example of the latter can be seen in Figure 5 as a prediction with low error located very close to an erroneous prediction. These anomalies exist since our method does depend upon the incoming data that could at instances be highly

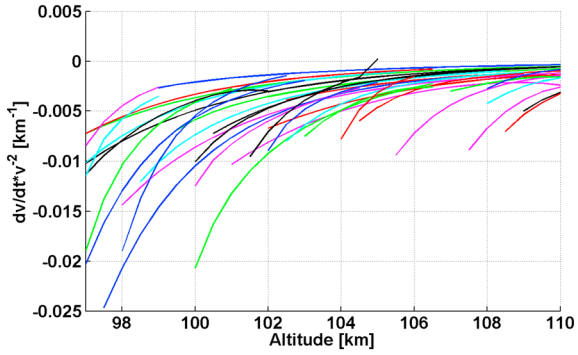

Figure 3. The $\frac{dV}{dt}\frac{1}{V^2}$ of meteoroids traveling at speeds > 40 km/s as detected by ALTAIR. Color coded similarly to that of Figure 2. Data are taken at 1600 UTC, DOY 131, 2007. Note an outlier measurement (black line) in the data at 105 km, but the methodology is able to ignore such erroneous measurements.

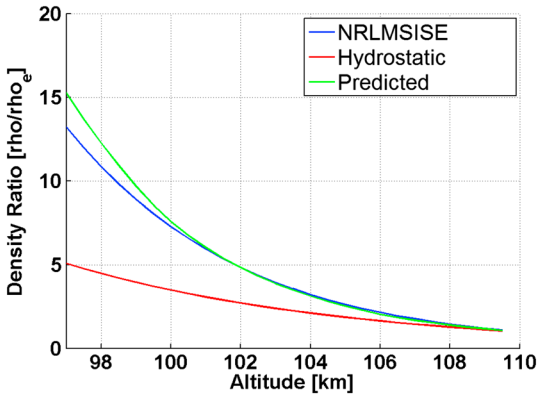

Figure 4. Density ratios calculated from minimization procedure with $\rho_{a,110\text{km}}$ as reference over 38 meteoroids. Reference altitude chosen at 110 km and ends at 97 km, due to the lower quantities of meteoroid data beyond these altitudes. Comparisons are made with NRLMSISE-00 and hydrostatic exponential models. Data are taken at 1600 UTC, DOY 131, 2007.

variable, especially if an insufficient amount of data is fed into the minimization process. Overall, the predictions tend to cluster together in such a way that we can calculate a meaningful average and standard deviation. As expected, the aforementioned average closely agrees with the prediction calculated from all data over the 20 min period.

If we desire the actual density values, we require statistics on the masses and bulk densities of the incoming meteoroids. If we refer to equation (18), we see that by measuring the variation across $\frac{dV}{dt}\frac{1}{V^2}\frac{\rho_{a,\text{ref}}}{\rho_a}$, it is equivalent to measuring the variation across $\frac{1}{R\rho_m}$. This is due to the fact that we take C_D constant across all meteoroids and we scale the measurements based upon one reference density. Figures 7 and 8 show this variation for two separate days. We scale the measurements relative to the median since it is less sensitive to outliers, especially since masses and bulk densities vary across 2 orders of magnitude between meteoroids. Based upon previous ALTAIR measurements, their respective median values are approximately $m = 1.36 \times 10^{-5}$ g and $\rho_m = 0.45\ \frac{g}{cm^3}$ [*Close et al.*, 2007, 2012]. The resulting estimated densities are shown in Figures 9 and 10.

It should be noted that although we have set the median to a specific value, there is still an uncertainty related to this value. This uncertainty can be minimized if we increase our sample size, but there is a theoretical limit as the median was derived from other parameters which are in turn uncertain as well (to be specific, the masses and bulk densities were derived from spherical scattering theory, which depends upon measurements of the integrated line density of the plasma created by the meteoroid [*Close et al.*, 2005]). In particular, detections made in VHF at ALTAIR are only sensitive to meteoroids of a certain mass range (6×10^{-6} g to 3×10^{4} g) [*Close et al.*, 2007], so our median must come from this particular source. We can also look at the median statistics per bin to gain a rough measure of this uncertainty, shown in Table 3. Note that σ_{median} is not the standard deviation of measurements about the median value but is instead the standard deviation of the median itself. From this we would expect roughly a 12% standard deviation on our density estimates, given that we know the statistics of the median as well as the velocities and accelerations perfectly. In comparison, we calculate from Figures 9 and 10 that the standard deviation is roughly 10%. Both these errors are associated with the methodology, as we assume that most meteoroids follow the given ablation and drag model. Note that additional error from inaccurate velocities and deceleration must be directly compounded here (the best case scenario being an additional 4% error).

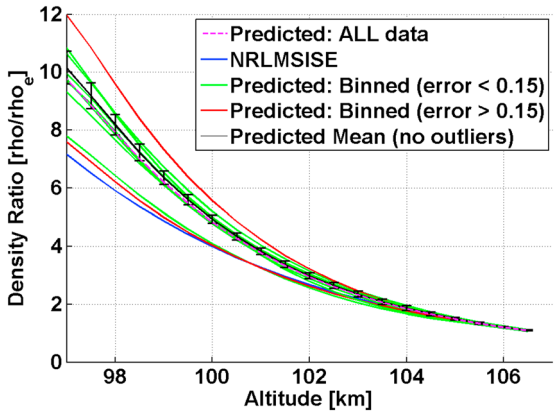

Figure 5. Density ratios as calculated at 1800 UTC, DOY 312, 2007, over nine bins from approximately 45 meteoroids per bin across 20 min. The mean estimate was calculated from all binned estimates possessing RMS error less than 0.15. The error bars indicate the standard deviation of these estimates (not including high error estimates but including false positive estimates).

Compared to NRLMSISE, the density ratios are much higher than expected, although the actual densities are more variable. Across the 2 days, we observe that the neutral density is significantly lower on the first day. However, NRLMSISE predicts that the densities across both days to be roughly equivalent. If we refer to the solar and geophysical

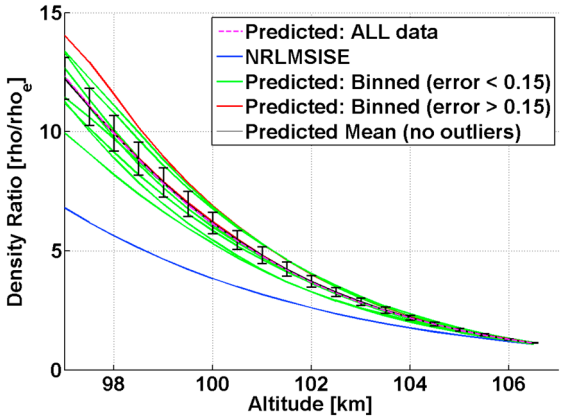

Figure 6. Density ratios as calculated at 1800 UTC, DOY 015, 2008, over nine bins from approximately 30 meteoroids per bin across 20 min. Same conditions as Figure 5 apply.

parameters (shown in Table 1), we see that on the second day, the $F_{10.7}$ and K_p indices are both greater compared to the first, possibly explaining the increase in neutral densities not reflected by NRLMSISE. Although these indices are included within NRLMSISE (in fact, NRLMSISE only exhibits a slight dependence on the $F_1$0.7 index and practically no dependence upon geomagnetic indices at these altitudes), the model does tend to predict the average behavior of the neutral densities and not phenomena on a shorter time scale (less than 1 day) [*Picone et al.*, 2002]. Furthermore, there could be other factors in the complex dynamics of the thermosphere that go unmodeled. Continuous measurements over multiple days would give us insight such that we can characterize geophysical variability across a longer time frame.

Another interesting analysis we can perform is on the computed ablation parameter D from the minimization process in Equation (12). Since meteoroids ablate in the free molecular flow regime ($Kn > 10$) at these altitudes, we can safely assume that $C_D = 2$ [*Popova*, 2004]. The histogram of $\frac{H*}{C_H}$ is shown in Figure 11. We infer here that C_H is variable across meteoroids, since if we take the often assumed $C_H = 1$ for free molecular flow, the corresponding H^* values tend to be too large in comparison to known materials. As well, approximately 10% of the estimates made for H^* are far too large, citing the possibility that these meteoroids do not follow our model and other physics is at work (variable ablation parameters, differential ablation, sputtering, etc.).

5. Conclusions and Future Work

We have in this paper gathered head echo data from ALTAIR at VHF frequencies to observe the head echoes of incoming meteoroids, measuring their position, velocity, and deceleration in 3-D. By analyzing large amounts of data, we utilize a minimization scheme such that we solve for the ablation parameters per meteoroid as well as the density ratios across different layers of the MLT region. If we are able to ascertain that the sporadic distribution of meteoroids does not change over time, we are also able to combine measurements across different days using the ratio distribution on the minimum order statistic such that we cancel the effects of changing neutral densities.

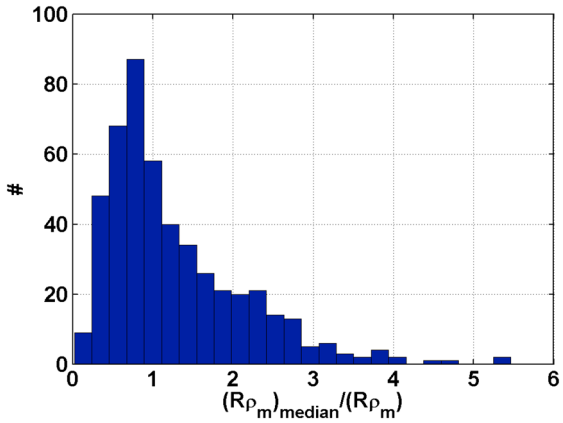

Figure 7. Variation of meteoroids ($R^{-1}\rho_m^{-1}$) scaled to median on 1800 UTC, DOY 312, 2007. The data reflect the total number of meteoroids across all bins.

To calculate the actual density values, we require further information regarding the properties of the meteoroids, particularly their masses, sizes, and bulk densities. Only two of these three properties are required such that we can compute the median value of $\frac{1}{R\rho_m}$. Note that there is an inferred dependence here on the method of observation, since different instruments might be sensitive to differing classes of meteoroids. Upon ascertaining the median meteoroid characteristics we can proceed to calculate the actual density values. The advantage here is that unlike traditional methods that seek to calculate the properties per meteoroid, we instead view the problem stochastically and associate it with a distribution. The method is shown to predict densities not captured by

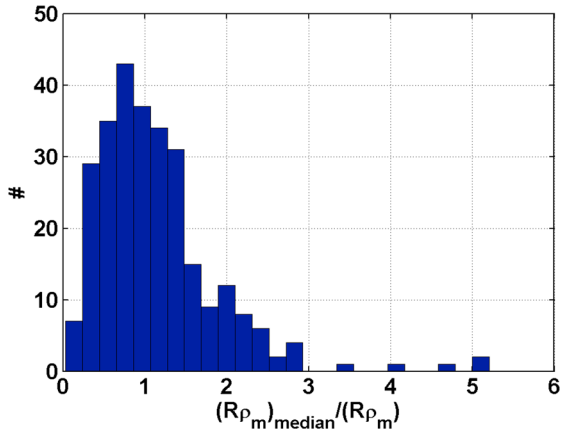

Figure 8. Variation of meteoroids ($R^{-1}\rho_m^{-1}$) scaled to median on 1800 UTC, DOY 015, 2008. The data reflect the total number of meteoroids across all bins. Note that on this day, there are less detected meteoroids as compared to day 312.

NRLMSISE and could give updates in real time regarding varying neutral densities. The focus here is that we are able to make estimations reflecting small-scale variations and physics at a certain location and time, as opposed to being on a global scale.

Because this method is mostly data driven, there is the dilemma of consistency across different sets of measurements. This is remedied by binning measurements over a longer period of time and evaluating each bin separately. Generally, the results tend to cluster together, showing approximately a 10% standard deviation across all predictions. The large error is attributed to the fact that meteoroid properties vary greatly from one another, often across several orders of magnitude. If we sample from an increasing number of meteoroids, we can decrease this error. This is, however, limited to the uncertainty regarding the median coupled with the measurement errors during detection. For example, if we know the median CDF, velocity, and deceleration very accurately, then sampling from 700 meteoroids can lower the error to approximately 4%.

Ultimately, there is still a dependence upon models within our work, particularly on the drag and ablation equations. Both equations hold the constants C_D, C_H, and H^* constant over time, which may not be true. Furthermore, we have assumed constant spherical meteoroids that ablate uniformly with no anomalous physics present (e.g., differential ablation and breakup). At least 10% of meteoroids do not conform to our models, evidenced by a small group of overly large $\frac{H*}{C_H}$ values that are unphysical.

Application of the proposed method at other HPLR sites does show promise if certain conditions are met. However, given the relative scarcity of these facilities and their narrow observation ranges, the method can only provide a local measure of dynamically changing neutral density. The measurements can be used to further improve atmospheric models locally or can serve as a benchmark for global atmospheric models at specific locations. Regarding the observations, there is no particular need for "down the beam" echoes (although these types of echoes do tend to last longer and possess better noise characteristics). It is, however, a necessity for accurate acceleration and velocity measurements in 3-D. More importantly, the sensitivity of the radar to specific frequencies and hence sizes of meteoroids must be known beforehand, such that the median of $R\rho_m$ can be accurately identified. This has no bearing upon the calculation of density ratios but is necessary for estimating actual densities. Finally, the beam pattern correction for the SNR is not critical but may provide additional information such as plasma properties, what stage the ablation process is at, and for filtering meteoroids outside the main beam.

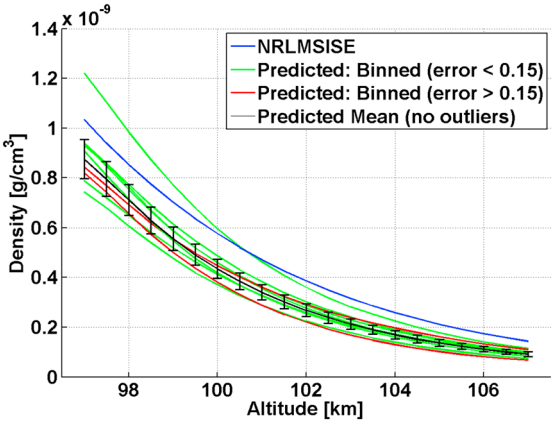

Figure 9. Densities as calculated at 1800 UTC, DOY 312, 2007, over nine bins from approximately 45 meteoroids per bin across 20 min. The mean estimate was calculated from all binned estimates possessing RMS error less than 0.15. The error bars indicate the standard deviation of these estimates (not including high error estimates but including false positive estimates).

Future work in this area include taking measurements during meteor shower events, as we can reduce the variability across individual meteoroids since they would originate from the same source. Although traditionally HPLA radars are more sensitive to sporadics,

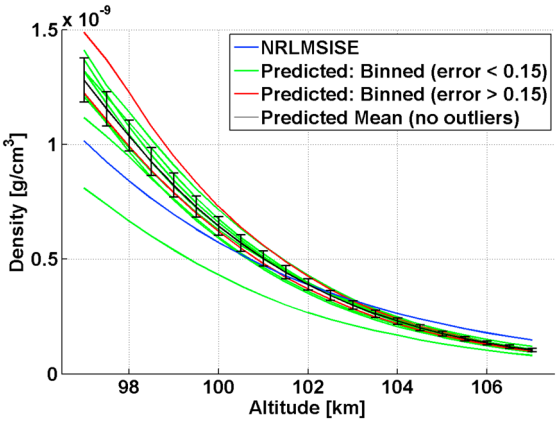

Figure 10. Densities as calculated at 1800 UTC, DOY 015, 2008, over nine bins from approximately 30 meteoroids per bin across 20 min. Same conditions as Figure 9 apply.

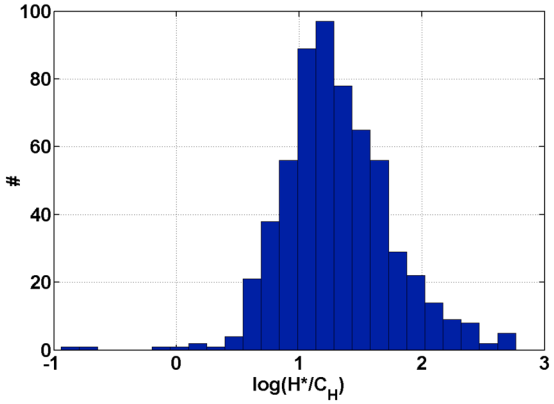

Figure 11. Histogram of estimated ablation parameters: $\log_{10}\left(\frac{H^*}{C_H}\right)$ is estimated from the minimization procedure over approximately 500 meteoroids. Data is taken at 1800 UTC, DOY 312, 2007.

Table 3. Statistics of $\frac{dV}{dt}\frac{1}{V^2}\frac{\rho_{a,\mathrm{ref}}}{\rho_a}$ Over Multiple Bins at 1800 UTC, DOY 312[a]

Bin	Median	σ_{median}	σ_{median} as %
1	9.882×10^{-4}	13.678×10^{-5}	13.8
2	8.639×10^{-4}	6.084×10^{-5}	7.0
3	8.607×10^{-4}	9.184×10^{-5}	10.7
4	8.677×10^{-4}	11.709×10^{-4}	13.5
5	6.750×10^{-4}	7.752×10^{-4}	11.5
6	8.206×10^{-4}	10.063×10^{-4}	12.3
7	10.011×10^{-4}	15.641×10^{-4}	15.6
8	5.802×10^{-4}	5.501×10^{-4}	9.5
9	7.628×10^{-4}	10.420×10^{-5}	13.7

[a]The standard deviation here corresponds to uncertainty in the median of meteoroid properties per bin. The last column indicates that this as a percentage, calculated as $\frac{\sigma_{\mathrm{median}}}{\mathrm{Median}} \cdot 100\%$. Red rows indicate bins where the mean squared errors of the estimate were large. Units in $\frac{1}{\mathrm{km}}$.

shower events have been observed [*Close et al.*, 2000; *Chau and Galindo*, 2008], and it is the hope that continued improvements in this area could lead to the use of our methodology for those data sets. Likewise, orbit analysis techniques for meteors could be employed such that we filter meteoroids from specific sources [*Kero et al.*, 2012; *Schult et al.*, 2013]. This would lead to less uncertainty regarding our statistics and hence better estimates overall. As well, we can take a more complex view regarding meteoroid ablation and introduce variable parameters. However, it should be noted that by doing so, we can potentially introduce too many degrees of freedom within our to-solve-for parameters, particularly if we require a model that can fit every observation. Ultimately, what we require is a model that fits most incoming meteoroids without being affected by outlying cases, such that the statistics of large numbers dictate the derivation of neutral densities.

Appendix A: Derivation for Ratio Statistics

The derivation here details the calculation of the distribution $(R\rho_m)$ if we are given data from multiple days under varying neutral density conditions. The major assumption here is that the meteoroids are IID with some unknown distribution for all days. Moreover, we must take the same number of N measurements per day. We start with equation (16) with the following substitutions: let $x = (R\rho_m)$, $y = (R\rho_m)_{mk}$, and $z = \frac{x}{y} = \frac{(R\rho_m)}{(R\rho_m)_{mk}}$. Thus, the quotient distribution can be written as

$$P(z) = \int_{-\infty}^{+\infty} |y| P_{x,y}(zy,\, y)\mathrm{d}y \tag{A1}$$

where $p_{x,y}$ is the joint probability distribution of independent variables x and y. However, since the variable zy is dependent on y, we expand equation (A1) to

$$P(z) = \int_{-\infty}^{+\infty} |y| P_x(zy|y) P_y(y)\mathrm{d}y \tag{A2}$$

We recognize the conditional probability $p_x\,(zy|y)$ can be expressed as

$$P_x(zy|y) = \frac{1}{1 - C_x(y)} H\,(x - y)\, P_x(zy) \tag{A3}$$

where H is the Heaviside function. Since y is the minimum and is positive in nature, we can remove the Heaviside function and absolute symbol from our equations. As well, we recognize that $P_y(y)$ is simply the probability of the minimum over N observations:

$$P_y(y) = NP_x(y)\left(1 - C_x(y)\right)^{N-1} \tag{A4}$$

Equation (A2) then becomes

$$P(z) = \int_{-\infty}^{+\infty} NyP_x(zy)P_x(y)\left(1 - C_x(y)\right)^{N-2}\mathrm{d}y \tag{A5}$$

Since we have the CDF instead of the PDF of z, we must integrate equation (A5):

$$C(z) = \frac{N}{N-1}\int_{-\infty}^{+\infty} F_x(zy)\cdot\frac{\mathrm{d}\left(F_x^{N-1}(y)\right)}{\mathrm{d}y}\mathrm{d}y + 1 \tag{A6}$$

where F_x is defined as the complement to the CDF:

$$F_x(x) = 1 - C_x(x) \tag{A7}$$

To solve equation (A6), we discretize accordingly:

let

$$z_i = r^{i-1}$$
$$y_i = (R\rho_m)_{\min} r^{i-1}$$

where

$$i = 1, 2, \ldots, m \tag{A8}$$

where r is the ratio of the geometric series. Usually, m is determined at a point such that $C(z_m) \approx 0$, although there is no consequence in letting m exceed this value. We then approximate equation (A8) as a summation:

$$C(z_j) - 1 = \frac{N}{N-1} \sum_{i=1}^{m} F_x(z_j y_i) \cdot \left[F_x(y_{i+1})^{N-1} - F_x(y_i)^{N-1} \right] \tag{A9}$$

Because we have abstracted the points of evaluation, we do not actually require the value of $(R\rho_m)_{\min}$. Equation (A9) can be manipulated into the matrix form seen in equation (17). While solving for F_x, it is useful to include the inequalities $F_{x,1} > F_{x,2} > \cdots > F_{x,m}$ and the equalities $F_{x,1} = 1$ and $F_{x,m} = 0$ due to the nature of a CDF. Note that because equation (A9) is an integral equation, we require a constant of integration to fully resolve the CDF to a specific point. This is later given as the median of meteoroid properties inferred from previous measurements.

For further details regarding the method of ratio statistics to predict the CDF, please refer to *Li and Close* [2015].

Acknowledgments
The authors would like to thank the FAA COE-CST for funding and support of this work. The data set used consists of meteoroid streak data as observed by ALTAIR, and although the data are not publicly available, it is available upon request at alanli@stanford.edu.

References

Akmaev, R. (2011), Whole atmosphere modeling: Connecting terrestrial and space weather, *Rev. Geophys.*, *49*, RG4004, doi:10.1029/2011RG000364.
Baldwin, B., and Y. Sheaffer (1971), Ablation and breakup of large meteoroids during atmospheric entry, *J. Geophys. Res.*, *76*, 4653–4668.
Bowman, B., W. Tobiska, F. Marcos, and C. Valladares (2008), The JB2006 empirical thermospheric density model, *J. Atmos. Sol. Terre. Phys.*, *70*, 774–793.
Briani, G., E. Pace, S. Shore, G. Pupillo, A. Passaro, and S. Aiello (2013), Simulations of micrometeoroid interactions with the Earth atmosphere, *Astron. Astrophys.*, *552*, A53, doi:10.1051/0004-6361/201219658.
Brown, P., S. Hunt, and S. Close (2001), Astronomical and physical data for meteoroids recorded by the ALTAIR radar, in *Proceedings of the Meteoroids 2001 Conference, Kiruna, Sweden, 6–10 Aug.*, edited by B. Warmbein, pp. 469–474, ESA Publ. Div., Noordwijk.
Champion, K., and F. Marcos (1973), The triaxial-accelerometer system on Atmosphere Explorer, *Radio Sci.*, *8*(4), 297–303.
Chau, J. L., and F. Galindo (2008), First definitive observations of meteor shower particles using a high-power large-aperture radar, *Icarus*, *194*, 23–29.
Chau, J. L., R. F. Woodman, and F. Galindo (2007), Sporadic meteor sources as observed by the Jicamarca high-power large-aperture VHF radar, *Icarus*, *188*, 162–174.
Clemmons, J., J. Hecht, D. Salem, and D. Strickland (2008), Thermospheric density in the Earth's magnetic cusp as observed by the streak mission, *Geophys. Res. Lett.*, *35*, L24103, doi:10.1029/2008GL035972.
Close, S., S. Hunt, M. Minardi, and F. McKeen (2000), Analysis of Perseid meteor head echo data collected using the Advanced Research Projects Agency Long-Range Tracking and Instrumentation Radar (ALTAIR), *Radio Sci.*, *35*(5), 1233–1240.
Close, S., M. Oppenheim, D. Durand, and L. Dyrud (2005), A new method for determining meteoroid mass from head echo data, *J. Geophys. Res.*, *110*, A09308, doi:10.1029/2004JA010950.
Close, S., P. Brown, M. Campbell-Brown, M. Oppenheim, and P. Colestock (2007), Meteor head echo radar data: Mass-velocity selection effects, *Icarus*, *186*, 547–556.
Close, S., R. Volz, R. Loveland, A. Macdonell, P. Colestock, I. Linscott, and M. Oppenheim (2012), Determining meteoroid bulk densities using a plasma scattering model with high-power large-aperture radar data, *Icarus*, *221*, 300–309.
Determan, J., S. Budzien, M. Kowalski, M. Lovellette, P. Ray, M. Wolff, K. Wood, L. Titarchuk, and R. Bandyopadhyay (2007), Measuring atmospheric density with X-ray occultation sounding, *J. Geophys. Res.*, *112*, A06323, doi:10.1029/2006JA012014.
Divine, N. (1993), Five populations of interplanetary meteoroids, *J. Geophys. Res.*, *98*(E9), 17,029–17,048.
Doornbos, E. (2012), *Thermospheric Density and Wind Determination From Satellite Dynamics*,1st ed., Springer, Berlin, doi:10.1007/978-3-642-25129-0.
Emmert, J. (2015), Thermospheric mass density: A review, *Adv. Space Res.*, *56*, 773–824.
Ghosh, A., and H. Y. J. McSween (1999), Temperature dependence of specific heat capacity and its effect on asteroid thermal models, *Meteorit. Planet. Sci.*, *34*, 121–127.
Grossmann, K., M. Kaufmann, and E. Gerstner (2000), A global measurement of lower thermosphere atomic oxygen densities, *Geophys. Res. Lett.*, *27*(9), 1387–1390.
Grun, E., H. Zook, H. Fechtig, and R. Giese (1985), Collisional balance of the meteoritic complex, *Icarus*, *62*, 242–272.
Hedin, A. (1987), MSIS-86 thermospheric model, *J. Geophys. Res.*, *92*(A5), 4649–4662, doi:10.1029/JA092iA05p04649.
Hey, J. S., S. J. Parsons, and G. S. Stewart (1946), Radar observations of the Giacobinid meteor shower, *Mon. Not. R. Astron. Soc.*, *107*, 176–183.
Holten, J. (2012), *An Introduction to Dynamic Meteorology*, vol. *88*, Academic Press, Amsterdam.
Jacchia, L. (1965), Static diffusion models of the upper atmosphere with empirical temperature profiles, *Smithsonian Contrib. Astrophys.*, *8*, 215–257.
Janches, D., J. Mathews, D. Meisel, and Q. Zhou (2000), Micrometeor observations using the Arecibo 430 MHz radar, *Icarus*, *145*, 53–63, doi:10.1006/icar.1999.6330.
Janches, D., S. Close, and J. Fentzke (2008), A comparison of detection sensitivity between ALTAIR and Arecibo meteor observations: Can high power and large aperture radars detect low velocity meteor head-echoes, *Icarus*, *193*, 105–111.
Janches, D., L. Dyrud, S. Broadley, and J. Plane (2009), First observation of micrometeoroid differential ablation in the atmosphere, *Geophys. Res. Lett.*, *36*, L06101, doi:10.1029/2009GL037389.
Kero, J., Y. Fujiwara, M. Abo, C. Szasz, and T. Nakamura (2012), MU radar head echo observations of the 2011 October Draconids, *Mon. Not. R. Astron. Soc.*, *424*, 1799–1806, doi:10.1111/j.1365-2966.2012.21255.x.

Li, A., and S. Close (2015), Mean thermospheric density estimation derived from satellite constellations, *Adv. Space Res.*, *56*, 1645–1657, doi:10.1016/j.asr.2015.07.022.
Love, S., and D. Brownlee (1993), A direct measurement of the terrestrial mass accretion rate of cosmic dust, *Science*, *262*(5133), 550–553, doi:10.1126/science.262.5133.550.
Loveland, R., A. Macdonell, S. Close, M. Oppenheim, and P. Colestock (2011), Comparison of methods of determining meteoroid range rates from linear frequency modulated chirped pulses, *Radio Sci.*, *46*, RS2007, doi:10.1029/2010RS004479.
Lyytinen, E., and M. Gritsevich (2016), Implications of the atmospheric density profile in the processing of fireball observations, *Planet. Space Sci.*, *120*, 35–42.
Mathews, J., D. Janches, D. Meisel, and Q. Zhou (2001), The micrometeoroid mass flux into the upper atmosphere: Arecibo results and a comparison with prior estimates, *Geophys. Res. Lett.*, *28*(10), 1929–1932.
Meier, R., U. Feldman, C. Brown, and J. Picone (1992), Absolute O and O_2 concentrations in the thermosphere from SKYLAB occultation data, *Planet. Space Sci.*, *40*(8), 1153–1166.
Nicolls, M., H. Bahcivan, I. Haggstrom, and M. Rietveld (2014), Direct measurement of lower thermospheric neutral density using multifrequency incoherent scattering, *Geophys. Res. Lett.*, *41*, 8147–8154, doi:10.1002/2014GL062204.
Offerman, D. (1974), Composition variations in the lower thermosphere, *J. Geophys. Res.*, *79*, 4281–4293, doi:10.1029/JA079i028p04281.
Opik, E. J. (1958), *Physics of Meteor Flight in the Atmosphere*, 1st ed., Interscience Publishers, New York.
Oppenheim, M., G. Sugar, E. Bass, Y. Dimant, and J. Chau (2008), Day to night variation in meteor trail measurements: Evidence for a new theory of plasma trail evolution, *Geophys. Res. Lett.*, *35*, L03102, doi:10.1029/2007GL032347.
Pardini, C., and L. Anselmo (2001), Comparison and accuracy assessment of semi-empirical atmosphere models through the orbital decay of spherical satellites, *J. Astronaut. Sci.*, *49*(2), 255–268.
Pellinen-Wannberg, A., and G. Wannberg (1994), Meteor observations with the European incoherent scatter UHF radar, *J. Geophys. Res.*, *99*, 11,379–11,390.
Picone, J., A. Hedin, and D. Drob (2002), NRLMSISE-00 empricial model of the atmosphere: Statistical comparisons and scientific issues, *J. Geophys. Res.*, *107*(A12), 1468, doi:10.1029/2002JA009430.
Popova, O. (2004), Meteoroid ablation models, *Earth Moon Planets*, *95*, 303–319.
Rogers, L., K. Hill, and R. Hawkes (2005), Mass loss due to sputtering and thermal processes in meteoroid ablation, *Planet. Space Sci.*, *53*, 1341–1354.
Schult, C., G. Stober, J. L. Chau, and R. Latteck (2013), Determination of meteor-head echo trajectories using the interferometric capabilities of MAARSY, *Ann. Geophys.*, *2013*, 1843–1851.
Shim, J., et al. (2012), CEDAR electrodynamics thermosphere ionosphere (ETI) challenge for systematic assessment of ionosphere/thermosphere models: Electron density, neutral density, N_mF_2, and h_mF_2 using space based observations, *Space Weather*, *10*, S10004, doi:10.1029/2012SW000851.
Simek, M., P. Pridal, P. Pecina, and J. Bocek (1997), Some aspects of meteoric head echo velocity determination, *Earth Moon Planets*, *77*, 1–17.
Strelnikov, B., M. Rapp, and F.-J. Lubken (2013), In-situ density measurements in the mesosphere/lower thermosphere region with the TOTAL and CONE instruments, in *An Introduction to Space Instrumentation*, edited by K. Oyma and C. Z. Cheng, pp. 1–11, TERRAPUB, Tokyo.
Vallado, D. (2013), *Fundamentals of Astrodynamics and Applications*, Microcosm Press, Hawthorne, Calif.
Vallado, D., and D. Finkleman (2014), Drag and energy accommodation coefficients during sunspot maximum, *Acta Astronaut.*, *95*, 141–165, doi:10.1016/j.actaastro.2013.10.005.
Vondrak, T., J. Plane, S. Broadley, and D. Janches (2008), A chemical model of meteoric ablation, *Atmos. Chem. Phys.*, *8*, 7015–7031.
Vronshten, V. (1983), *Physics of Meteoric Phenomena*, D. Reidel, Dordrecht, Holland.